Structural Analysis of Historical Constructions – Modena, Lourenço & Roca (eds)
© 2005 Taylor & Francis Group, London, ISBN 04 1536 379 9

Structural analysis of Küçük Ayasofya Mosque in İstanbul

M. Massanas, P. Roca & M. Cervera
Universitat Politècnica de Catalunya, Barcelona, Spain

G. Arun
Yildiz Teknik Üniversitesi, İstanbul, Turkey

ABSTRACT: The paper describes a preliminary structural analysis of Küçük Ayasofya Mosque in İstanbul carried out by means of a continuum damage formulation specifically developed for the study of large buildings made of brittle material such as masonry. A discussion of the results obtained in the simulation of different actions such as gravity loads, differential settlements and earthquake, is presented.

1 INTRODUCTION

The Küçük Ayasofya Mosque, the former Church of Sts. Sergius and Bacchus, is a Byzantine construction built during 527–536 A.D. in İstanbul. It consists of an octagonal nave enlarged by four semi-circular niches surrounded by a two-storey ambulatory. The octagonal nave is covered by la large ribbed dome consisting of 16 shell sectors combining alternately concave and flat surfaces.

The building is showing significant structural disorders such as large deformations at the piers and at the dome and important cracks across the vertical walls and dome surfaces. Due to its historical interest– together with the concern generated by its current damaged condition – Küçük Ayasofya has deserved attention from different researchers and some studies are now available (Özsen and Bairam, 1995, on the structure, Aköz and Yüzer, 1995, on material properties, Arun, 2001, on survey, Yüzügüllu and Durukal, 1997, on the effects of train traffic, or Alkiş et al., 2003 on the deformations of the building). However, a more detailed and general assessment is still needed in order to accurately evaluate its structural condition, characterize active processes causing deterioration and define possible repair or strengthening actions. Surveillance carried out during the last years has shown that, although most of the lesions exhibited by the building are very ancient, the opening of some of the cracks is still progressing.

The present paper describes a preliminary structural analysis of Küçük Ayasofya Mosque carried out by means of a formulation based on the mechanics of continuum damage. This formulation was specifically developed for the study of large buildings made of brittle materials such as masonry and has already been used for the analysis of historical constructions (Roca, 2001).

The study consists of the simulation of different actions (gravity, soil settlements and earthquake) and is aimed at the characterization of their possible effects on the building. The analysis focuses on the possible contribution of such actions to the generation of the main observable lesions. This paper presents preliminary results obtained for a partial model elaborated from the information available on geometry and materials of the building.

2 DESCRIPTION OF THE BUILDING

The construction of the Church of the Sts. Sergius and Bacchus started at the beginning of the Justinian mandate, about the year 527 and was finished before the year 536. It was built as the basilique of the Palace of Hormisdas, the residence of Justinian in Constantinople as the heir to the throne. The building was placed in an irregular space between the palace and the church of the Sts. Peter and Paul, with which it shared the nartex, atrium and propileum (Krautheimer, 1965). From 1504 on, after the Ottoman conquer of Constantinople, the building has been used as a mosque with the new name of Küçük Ayasofya Camii; except for the West main entrance, of Ottoman style, the rest of the building, the main architectural components of the inner structure (the dome, piers and niches) are original and have only been subject to minor decorative alterations.

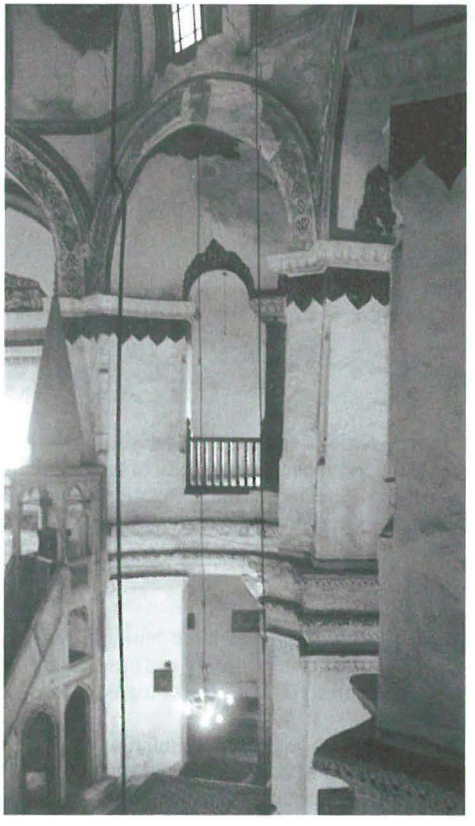

Figure 1. Deformation of piers.

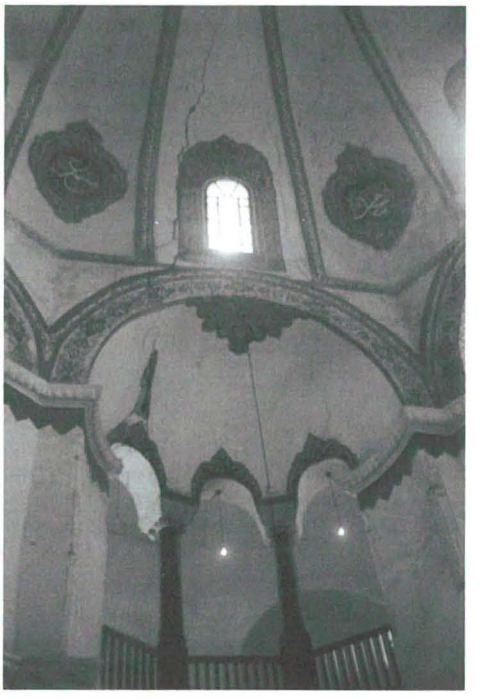

Figure 2. Cracking of the dome and semi-circular spandrels.

Figure 3. View of the interior.

The building has experienced a number of accidents across its life, among them the fire of 1758 and numerous important earthquakes. Several parts of the building have been reconstructed due to the destruction caused by the latter, or other possible actions; this is the case of most of the external walls and ambulatories with the exception of some sectors of the North wall.

During 1870–1871 a main railway line was built only a few meters apart from the South-West wall of the building. Later, from 1950 to 1960, the platform of the railway line was elevated to 2.5 m above the ground level of the building; this modification meant the formation of a new embankment in part retained by the South wall itself.

During most of the 20th century (if not during most of the entire life of the building), lack of maintenance has contributed very much to the deterioration of the dome. Water filtration was affecting the dome until a lead cover was provided to the roof in 1970. The roof is currently being restored.

The structural damage shown by the structure of Küçük Ayasofya Mosque (Figs. 1–3) is possibly connected to some of the above mentioned facts. Among other existing lesions, important cracks affecting the nave, the semi-circular niches and the ambulatory are observed. Figure 4 describes the main cracks experienced by the dome and the semi-circular spandrels of the South-East quadrant. Five different crack systems (numbered 1 to 5 in Figure 4) can be seen close to the crown of the arch of the apse (1), along the shell sector over the pier (2), in the semi-circular spandrel of the niche and then across the upper shell sector (3),

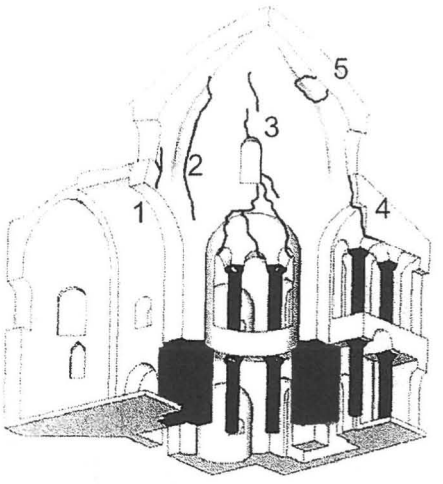

Figure 4. Main cracks exhibited by the inner structure at the Souh-West quadrant.

across the lateral spandrel and arch (4) and, more locally, at the centre of a shell sector (5). The walls of the tambour are severely affected by cracks 1–4, which can also be seen from their external paraments.

Similar cracks also exist in the North-East and South-West quadrants, and, although less developed, in the North-West quadrant. According to Alkis et al. (2001), further opening of the main cracks has been measured during last years.

Significant horizontal drifts, amounting up to 40 cm, have been also measured at the piers by Alkis et al. (2001). Such movements point to a general deformation of the building towards the South-West direction.

3 TENSION-COMPRESSION DAMAGE MODEL

In the present work, an isotropic damage model, with two scalar internal variables to monitor the local damage under tension and compression, is used. This provides a simple constitutive model which, nevertheless, is able to capture the overall non-linear behaviour including strain hardening/softening response, stiffness degradation and regradation under multiple stress reversals. Furthermore, the model can be implemented in a strain-driven form which leads to an almost closed-form algorithm to integrate the stress tensor in time. This is a most valuable feature for a model intended to be used in large-scale computations. It must be noted, however, that some specific aspects of the response of brick or stone masonry, such as anisotropy due to bed joints, are not yet included in the model.

The Continuum Damage Mechanics Theory (CDMT) is based on the definition of the effective stress ($\bar{\sigma}$) concept, which is assumed to be the stress associated with the strains under undamaged state. In order to simulate two different behaviours in tension and compression, a split of the (second-order) effective stress tensor into tensile ($\bar{\boldsymbol{\sigma}}^+$) and compressive ($\bar{\boldsymbol{\sigma}}^-$) components is needed. The constitutive equation obtained, after including two internal-like variables, namely tensile (d^+) and compressive (d^-) damage variables, is the following:

$$\boldsymbol{\sigma} = \left(1-d^+\right)\bar{\boldsymbol{\sigma}}^+ + \left(1-d^-\right)\bar{\boldsymbol{\sigma}}^- \tag{1}$$

These damage variables indicate the level of damage reached at each Gauss point: $d^{\pm}=0$ for undamaged material and $d^{\pm}=1$ for totally collapsed material. Notice that a tensile-damaged material would have its original – undamaged – behaviour if the stress state changed to compression, and vice versa, due to the definition of two different damage variables. In order to permit the comparison of different 3D states to define concepts such as loading, unloading, or reloading, a scalar positive quantity, termed as *normalized equivalent stress norm*, is defined. As a consequence of the stress split, two separate norms are necessary: tensile norm τ^+ and compressive norm τ^-. In the present work, the following form will be assumed:

$$\tau^{\pm} = \frac{1}{f_e^{\pm}}\left(\bar{\boldsymbol{\sigma}}^{\pm} : \mathbf{C}^{\pm} : \bar{\boldsymbol{\sigma}}^{\pm}\right)^{1/2} \tag{2}$$

where the non-dimensional four order metric tensors $\mathbf{C}^+$ and $\mathbf{C}^-$ are identical, and equal to the inverse of the (normalized) elastic tensor. The normalizing factors f_e^+ and f_e^- represent the values of the tensile and compressive uniaxial stresses that define the onset of damage under uniaxial tension and compression, respectively.

With the above definitions, two separated damage criteria, g^+ and g^- are introduced:

$$g^{\pm}\left(\tau^{\pm}, r^{\pm}\right) = \tau^{\pm} - r^{\pm} \le 0 \tag{3}$$

Variables r^+ and r^- are normalized internal strain-like variables, which can be interpreted as current damage thresholds, in the sense that their values control the size of the (monotonically) expanding damage surfaces. Due to their normalized nature, the initial values are unitary $r_0^+ = r_0^- = 1$. In this sense, the explicit definition of the current values of the internal variables has the form:

$$r^{\pm} = \max\left[r_0^{\pm}, \max\left(\tau^{\pm}\right)\right] \tag{4}$$

Finally, the damage indices d^+ and d^- are explicitly defined in terms of the corresponding current values of the damage thresholds, so that they are monotonically increasing functions such that $0 \leq d^{\pm}\left(r^{\pm}\right) \leq 1$. These damage functions can be expressed according to the behaviour that is desired to simulate. For example, linear hardening/softening behaviour would have the following expression:

$$d^{\pm}\left(r^{\pm}\right) = \left(1 - H_d^{\pm}\right)\left(1 - \frac{r_0^{\pm}}{r^{\pm}}\right) \tag{5}$$

where $H_d^{\pm}$ is a constant, defined as a material property, different for tension and compression. In case of softening ($H_d^{\pm} < 0$), this parameter must be related to the *fracture energy* G_f of the material, and to the *characteristic length* of the finite element mesh, to ensure mesh-size objective results. More details on the formulation can be found in Cervera (2003).

4 STRUCTURAL MODEL

It must be noted that the structure does not show perfect lateral symmetry due to the overall irregularity of its plan. Due to this, an accurate analysis would require a complete modelling of the entire building. As a first step, the preliminary study here presented has been carried out on a simpler model consisting of a quadrant of the building (Fig. 5). The South-East quadrant has been selected for this purpose. The model includes 230,000 tetrahedral solid elements with maximum dimension of 0.5 m in walls and dome, 0.4 m in piers and 0.1 m in columns (Fig. 5). All structural elements include at least 4 tetrahedral elements across their minimum dimension.

Based on the information available on the materials, only four different sets of material properties have been defined for, respectively, the stone of the monolithic columns in niches sand ambulatory walls, the stone masonry of the main piers, the brick masonry of vaults and dome and the masonry of walls. The latter consists of brick masonry stiffened with stone blocks of different nature (limestone, argillaceous limestone and travertine) embedded in 4–5 cm thick mortar beds.

A compressive strength (f_c) of 30 N/mm^2 and a density (γ) of 25 kN/m^3 has been defined for the stone columns. The corresponding values considered for the both the brick or brick and stone masonries are $f_c = 4.5$ N/mm^2 and $\gamma = 18$ kN/m^3. A Young modulus of $1000 \cdot f_c$ and a Poisson coefficient of 0.2 have been defined for all materials. The tensile strength has been estimated as $0.07 \cdot f_c$ in the case of stone and masonry stone and $0.05 \cdot f_c$ for brick masonry.

Future studies should consider a more detailed distinction among the different materials and masonries, together with a more accurate estimation of the different material properties; this, in turn, requires further research on the existing materials and their mechanical properties.

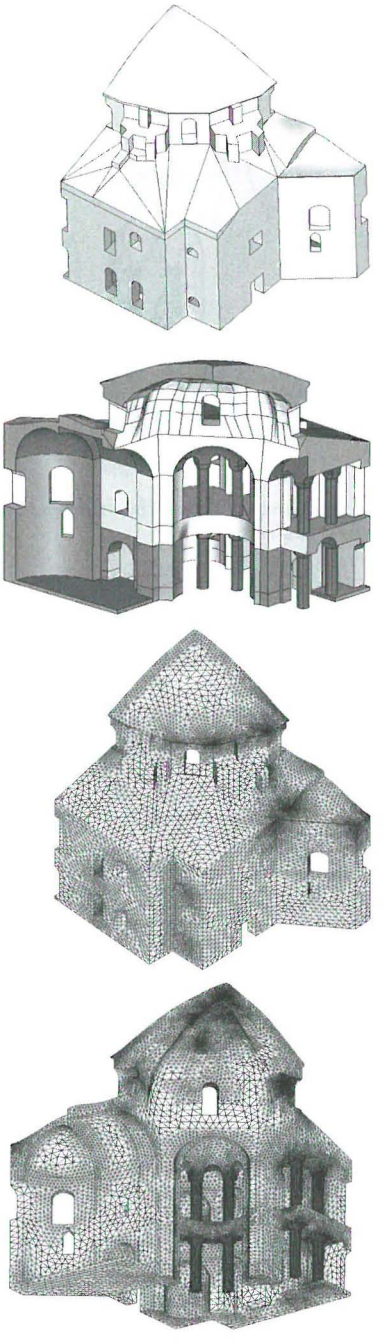

Figure 5. Geometry of structural model and FE mesh.

5 SIMULATION OF DIFFERENT ACTIONS

5.1 *Dead loading*

The model has been first used to analyze the resulting distribution of stresses and damage caused by the only effect of the dead load. A conventional instantaneous analysis, with all dead loading simultaneously applied, has been performed for that purpose. Figures 6a and 6b respectively show the distribution of the tensile ratio and the maximum compression stresses obtained for the analyzed quadrant.

Dead loads produce mostly compression stresses across the structure. However, cracking develops at mid-span of the apse arch, where the tension ratio reaches a value above 1 (with maximum of 1.6). Moderate tensile stresses appear at the spandrels of the semi-circular niches, with tensile ratio up to 0.6 (maximum tension stress of 0.14 N/mm^2).

In the rest of the structure, the distribution of compression is far from being uniform. Although most of the walls and shell sectors reach average compression values within 0.2 to 0.4 N/mm^2, several regions exist showing maximum compression stresses below 0.015 N/mm^2. These regions include all the spandrels existing below the windows of the tambour. As expectable, these windows prevent the arches from receiving a significant part of the load of the dome by forcing the deviation of the vertical compression forces towards the piers. This effect can be described as the generation of a set of relieving arches within the dome, which spring from the piers and rise to the region above the windows. The region below the relieving arches is subjected to very low confinement and is thus likely to experience cracking, in the long term, due to the contribution of other possible actions.

According to the analysis (and for the material properties considered), the piers experience only very little horizontal displacements between 0.2 and 0.3 mm. As something expectable (but to a remarkable extend), the instantaneous analysis can not predict large deformations such as those actually shown by the building. However, a very significant, long-term amplification of these deformations is conceivable across a long historical period. In fact, large deformations affecting piers, buttresses and other structural components are commonly observed in ancient constructions. In many cases, such large deformations are one or more orders of magnitude superior to those that can be predicted by instantaneous or short-term numerical analysis, even if non-linear material or geometrical effects, or even a conventional treatment of primary creep at short or mid-term, are considered. Different actions and phenomena occurring during the construction process and also during the long-term, historical life of the building, such as repeated low-intensity earthquakes, thermal or hygrometric cycles, or long-term damage related to creep, may have contributed very significantly to increase the overall deformation of the structure. Since the more persistent action is gravity, it is not strange that the increase of deformation manifests as a monotonic, non-assimptotic amplification of the initial deformed shape due to dead load.

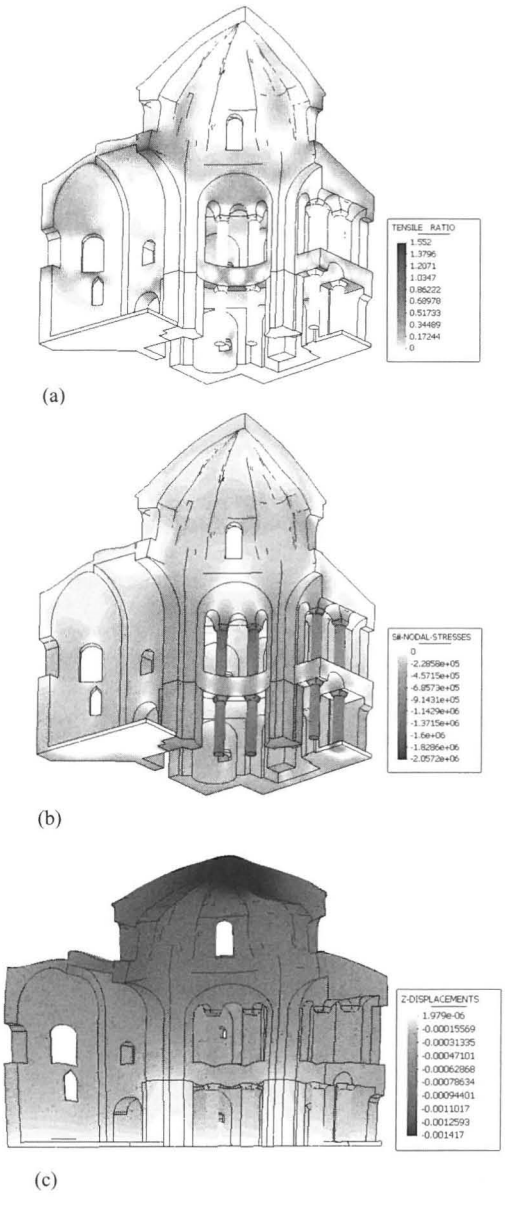

Figure 6. Distribution of (a) the tensile ratio, (b) maximum compression stresses in N/m^2 and (c) deformations, for gravity loading.

5.2 *Differential column-to-pier settlements*

Two types of differential settlements are likely to have affected the building. On the one hand, the dominant drift toward the South-East direction suggest the possibility of an overall soil deformation increasing towards the railway line existing close to the perimeter of the building; this settlement is possibly due to soil consolidation caused by the railway embankment and traffic.

Second, more local differential settlement may have occurred among the different vertical components of the building, that is to say, among columns, piers and walls, due to the very different average compression stresses supported by them; the average compression stresses carried by these elements, according to the analysis described in section 5.1, are 0.3, 0.7 and 1.2 N/mm^2 respectively.

At the moment, and due to the lack of detailed geotechnical information and measurements, only the effect of differential settlements between piers and columns has been tentatively analyzed. The analysis, consisting of the simulation of a gradually increasing vertical settlement affecting only the columns, has shown that a vertical displacement of only 1.5 mm is enough to cause in them intense tensile stresses. In practice, no cracking in the monolithic stone columns should be expected, but just a (partial) loss of the contact between these and the above spandrels, at the existing joints; this partial separation will produce, in turn, the partial (or even total) unloading of both the columns and spandrels.

To allow further speculation on this possibility, a complementary analysis has been carried out on a modified model with no monolithic columns (Fig. 7). In this second model, the spandrels experience expectable, but moderate tension stresses below the assumed tensile strength (maximum tension ratio of 0.7), showing that a initial equilibrium might be possible even if the columns where in fact not contributing to sustain a significant part of the weight of the spandrels and dome.

Even if the tensile stresses experienced by the spandrels in this hypothesis are moderate, damage (in the form of severe cracking and local deterioration) should be expected at the long-term due to the contribution of additional actions (as already mentioned, repeated minor earthquakes or thermal cycles) and the unconfined state of masonry. Thus, the hypothesis of the partial unloading of the columns helps to explain the appearance of crack (4) in Figure 4 as mainly caused by the long-term effect of gravity loading.

5.3 *Seismic response*

As a first approach, the effect of the seismic action has been modeled by a set of static equivalent loads distributed according to the mass. Different calculations have been carried out with the horizontal loads applied along the +x, −x, +y, −y axes, with the x and y axes respectively oriented in the longitudinal (façade-apse) and the transverse directions of the nave (Fig. 8). Given the seismicity of İstanbul and the long life-span of the building, the static equivalent loads have been calculated for an acceleration of a = 0.3 g. These forces are gradually applied on the building in a second step, after the application of the dead load, so that they act, in fact, on an initial condition subject only to the very moderate damage described in section 5.1.

In a simplified way, and defining approximate boundary conditions, the analysis is carried out on the one-quarter model of the building. It must be mentioned that, given the non-linearity of the problem, carrying out an accurate analysis requires a more complete model involving at least one half of the building.

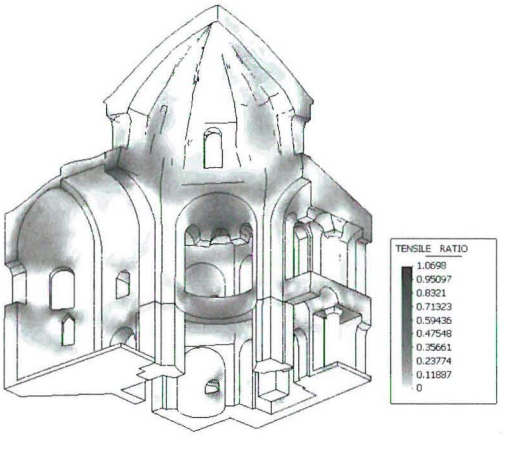

Figure 7. Distribution of the tensile ratio for gravity loading in the modified model.

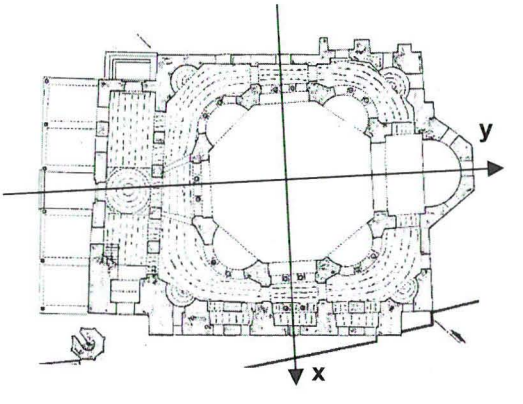

Figure 8. Directions "x" and "y" of horizontal forces applied in the analyses.

Figures 9a and 9b show the obtained distribution of tensile ratio. For forces acting in −x direction, the calculation predicts the appearance of significant tensile damage (tensile ratio above 1) in the crown of the apse arch, the semicircular spandrels and upper region of the dome in the case of forces acting in the −x direction. Tensile damage is predicted in the semicircular and lateral spandrels over columns and sector shells located over the piers for forces acting in the −y direction. Additional, intense but localized damage appears in the lintels over the columns and window arches. Most of the damage appears in regions which the analysis for dead load showed to be particularly sensitive (as those related to cracks 1–4 in Figure 4). In particular, a moderately damaged region, appearing for forces applied both in the −x and −y directions, can be related with the vertical crack existing along the intersection of the flat surfaces of the shell sector over the pier (crack 2 in Figure 4). Severe damage (with high tensile ratio) is experienced in regions located below the windows of the tambour, as the semicircular spandrels and lateral arches which close the apse and ambulatory.

A maximum compression ratio of 0.56 is obtained in the analyses, meaning that no damage related to compression stresses is produced.

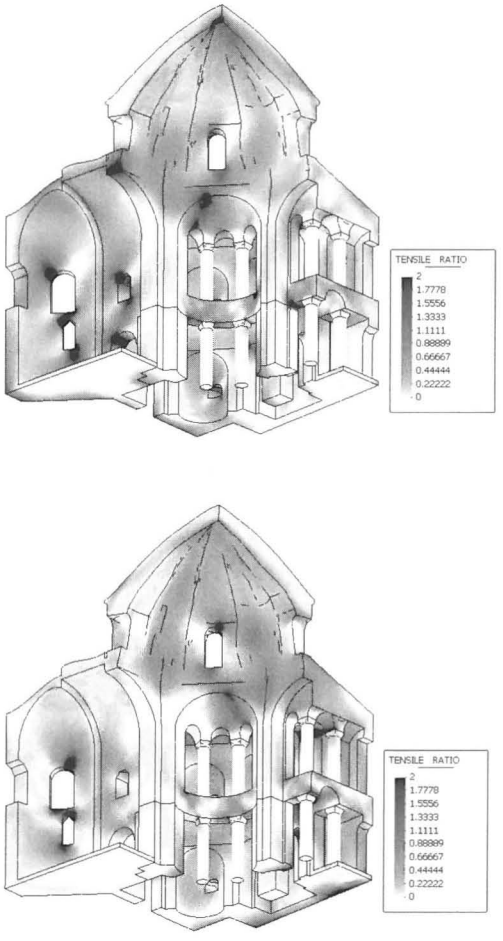

Figure 9. Distribution of tensile damage for seismic forces applied in the −x (above) and −y (below) directions (zones damaged in tension correspond to tensile ration ≥ 1.

6 CONCLUSIONS

A preliminary analysis of Küçük Ayasofya Mosque in İstanbul has been undertaken based on a tension-compression damage FE formulation. The analysis, carried out on a structural model comprehending a quadrant of the structure, has allowed a certain insight on the effect of different actions (dead loads, local pier-column differential settlements and earthquake) and their possible contribution to cause the main lesions shown by the building.

The authors intend to continue the study after the extension of the formulation to new capabilities now in development (such as dynamic analysis in the time-domain).

A more complete structural model, comprehending the entire construction, is also needed to account for the influence of the remarkable construction irregularities and to allow an accurate seismic analysis. A more detailed model would require, in turn, more information available on the geometry, materials and historical actions having affected the construction. Significant actions for the building, such as traffic on the close railway line or the overall soil settlements, are still to be analyzed.

REFERENCES

Aköz, F., Yüzer, N, 1995, Investigation of material properties of Küçük Ayasofia Mosque – The Church of Sts. Sergios and Bacchus in İstanbul.*Architectual Studies of Historical Buildings IV*, Southhampton: Computational Mechanics Publications.

Alkiş, A., Demirel, H., Doğan, U., Düpe, R., Gerstenecker, C., Krocker, R., Arun, G., Snitil, B., 2001, Deformation Observations at the church of Sergios and Bacchus by Photogrammetric Tools. *Studies in Ancient Structures*, İstanbul: Yıldız Technical University.

Arun, G., 2001, Investigations on Küçük Ayasofia Mosque-The Church of Sts. Sergios and Bacchus in İstanbul. *On-site Control and Evaluation of Masonry Structures*, Bagneux: Rilem publications s.a.r.l.

Cervera, M., 2003, *Viscoelasticty and Rate-dependent Continuum Damage Models*. Pub. M79, Barcelona: Center for Numerical Methods in Engineering.

Krautheimer, R., 1984, *Early Christian and Byzantine Architecture.* Pelican History of Art Series. 4th ed.: Yale Univ.

Özsen, G.A., Bairam, E., 1995, Structural evaluation of the dome of Küçük Ayasofya – Sts. Sergius and Bacchus. *Architectual Studies of Historical Buildings IV*, Southhampton: Computational Mechanics Publications.

Roca, P., 2001, Studies on the structure of Gothic cathedrals. *Structural Analysis of Historical Constructions III.* Guimaraes: Universidade do Minho.

Yüzügüllu, Ö, Durukal, E. 1997, The effects of Train Traffic on the Küçük Ayasofya Mosque in İstanbul. *Studies in Ancient Structures*, İstanbul: Yıldız Technical University.